UNIVERSITY OF HELSINKI

https://helda.helsinki.fi

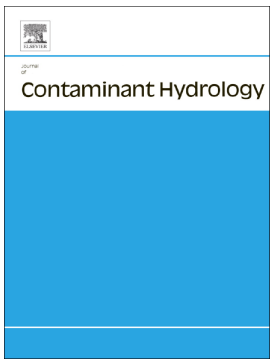
Sorption of selenium species onto phlogopite and calcite surfaces : DFT studies

Puhakka, Eini; Li, Xiaodong; Ikonen, Jussi; Siitari-Kauppi, Marja

2019-12
Elsevier B.V.
http://hdl.handle.net/10138/334264
Puhakka, E, Li, X, Ikonen, J & Siitari-Kauppi, M 2019, 'Sorption of selenium species onto phlogopite and calcite surfaces : DFT studies', Journal of Contaminant Hydrology, vol. 227, 103553, pp. 1-10. https://doi.org/10.1016/j.jconhyd.2019.103553

Downloaded from Helda, University of Helsinki institutional repository. https://helda.helsinki.fi
This is an electronic reprint of the original article.
This reprint may differ from the original in pagination and typographic detail.
Please cite the original version.

Journal Pre-proof



Sorption of selenium species onto phlogopite and calcite surfaces: DFT studies

Eini Puhakka, Xiaodong Li, Jussi Ikonen, Marja Siitari-Kauppi

PII: S0169-7722(19)30068-3

DOI: https://doi.org/10.1016/j.jconhyd.2019.103553

Reference: CONHYD 103553

To appear in: *Journal of Contaminant Hydrology*

Received date: 6 March 2019

Revised date: 10 September 2019

Accepted date: 10 September 2019

Please cite this article as: E. Puhakka, X. Li, J. Ikonen, et al., Sorption of selenium species onto phlogopite and calcite surfaces: DFT studies, *Journal of Contaminant Hydrology*(2018), https://doi.org/10.1016/j.jconhyd.2019.103553

This is a PDF file of an article that has undergone enhancements after acceptance, such as the addition of a cover page and metadata, and formatting for readability, but it is not yet the definitive version of record. This version will undergo additional copyediting, typesetting and review before it is published in its final form, but we are providing this version to give early visibility of the article. Please note that, during the production process, errors may be discovered which could affect the content, and all legal disclaimers that apply to the journal pertain.

© 2018 Published by Elsevier.

Journal Pre-proof

Sorption of selenium species onto phlogopite and calcite surfaces: DFT studies

Eini Puhakka, Xiaodong Li, Jussi Ikonen, Marja Siitari-Kauppi*

Department of Chemistry, P.O. Box 55, FI-00014 University of Helsinki, Finland

*Corresponding author and contact e-mail: xiaodong.li@helsinki.fi

Abstract

Sorption of Se(IV) and Se(VI) species onto Mg-rich biotite (phlogopite) and calcite surfaces was investigated using molecular modelling techniques. A CASTEP code implemented into Materials Studio was used to calculate the periodic systems, site densities and site types on the phlogopite and calcite surfaces. According to the results, the Se oxyanions attach to both edge and basal surfaces of phlogopite via an oxygen atom. However, calculated sorption energies indicate that surface complexation reactions via hydrogen bonding happen on the edge surfaces of phlogopite while cation exchange reactions happen on the basal surfaces of phlogopite. These reactions occur on the so-called weak sites according to the PHREEQC modelling. On the calcite surface, only cation exchange reactions are possible, and only for neutral Se species which do not occur in low saline groundwater conditions with pH 8-10. Biotite which is an abundant mineral in crystalline rock works fairly well as a sorbent but calcite which often exists on fracture surfaces of bedrock does not act as a sorbent for Se species.

Keywords: sorption, selenium, biotite, phlogopite, calcite, DFT

1. Introduction

In Finland and Sweden, the final disposal of spent nuclear fuel is considered to take place in deep geological repositories surrounded by bedrock according to the KBS-3 multiple barrier concept

in stable granitic-type rock formations (Geier et al., 2012; Posiva Oy, 2012). This repository system has been designed to isolate the harmful radionuclides and to prevent their migration into the groundwater system in the case of a release of radionuclides from the repository (Poteri et al., 2014). Once released, the migration of the radionuclides in flowing groundwater will be delayed by two processes, diffusion into the rock matrix and sorption onto fracture and mineral surfaces (Ewing, 2015; Grisak and Pickens, 1980; Neretnieks, 1980; Séby et al., 1998).

One of the crucial radionuclides that might be released from the repository is Se-79 which has a long half-life of around 3.7×10^5 years. Therefore, it has a high impact on the cumulative radioactive dose in a nuclear waste repository (Atwood, 2010; Lehto and Hou, 2011). Furthermore, it has complicated redox chemistry and high mobility in groundwater, which makes it one of the radionuclides that is of great concern for the long-term safety of radioactive waste repository (Ikonen et al., 2016b; Li et al., 2018; Yang et al., 2018). Concerning the selenium species, selenate (SeO_4^{2-}) or Se(VI) is the most soluble and mobile species, whereas selenite (SeO_3^{2-}) can be slightly sorbed to oxide surfaces, and neutral Se^0 is immobile under anoxic conditions (Boult et al., 1998; Duc et al., 2003; Lehto and Hou, 2011).

Selenate dominates the selenium species under oxic conditions in natural waters (Lehto and Hou, 2011). Sorption of selenate onto mineral surfaces usually occurs as a weakly-bounded outer sphere mechanism where no direct chemical bonding exists (De Cannière et al., 2010), and the distribution coefficient (K_d) of selenium is much lower than strongly sorbing radionuclides found in spent nuclear fuel like caesium (Muuri et al., 2017; Söderlund et al., 2016; Tsai et al., 2009), barium (Muuri, 2015) and strontium (Eikenberg et al., 1994; Vilks and Degueldre, 1991). Under anoxic conditions i.e. lower redox potentials, selenium is found to be in oxidation state +IV, and the dominant species is biselenite ($HSeO_3^-$) in the potential range of 200 – 400 mV at pH 7, and

selenite (SeO_3^{2-}) in the range of 100 – 300 mV at pH 9 (Lehto and Hou, 2011). The sorption mechanism of these species was found to be inner sphere complexation where a direct chemical bond is formed between an oxygen atom from the oxyanion and a structural surface metal atom (Martínez et al., 2006; Missana et al., 2009b). Sorption of $HSeO_3^-$ is more favourable than that of SeO_3^{2-}, because the loss of water during the reaction with $HSeO_3^-$ is energetically easier than the expulsion of a hydroxyl group from the surface in the reaction of SeO_3^{2-} (Hayes et al., 1987). This reaction mechanism is analogue to the nucleophilic S_N2-i substitution reaction detected in organic chemistry (Chubar et al., 2005).

Olkiluoto has been selected as the final disposal site for nuclear waste repository in Finland. Biotite, the Mg-endmember of which is phlogopite, is a common mineral in gneisses and other bedrock types found in Olkiluoto site. Calcite, on the other hand, is a typical fracture filling and coating mineral found in Olkiluoto site (Aaltonen et al., 2016). Biotite is also one of the main minerals of the granodiorite in the Grimsel Test Site in Switzerland where post-metamorphic reginal uplift is still ongoing (Möri et al., 2003; Tachi et al., 2015) and calcite is a typical mineral in the metamorphic rocks, and it is also a general filling material in joints. Extensive studies have been performed under both in-situ and laboratory conditions with rocks containing these two minerals (Ikonen et al., 2016b, 2016a; Jokelainen et al., 2013; Soler et al., 2015). However, there is still little information about the sorption sites of these two minerals nor the mechanisms of selenium sorption when interpreting the experimental sorption results. The sorption of selenium species on biotite or calcite was normally ascribed to a surface complexation mechanism involving two types of surface hydroxyl groups, the strong sorption sites ($\equiv S^SOH$) and weak sorption sites ($\equiv S^WOH$) (Ervanne et al., 2016; Li et al., 2018; Missana et al., 2009a). Moreover, it is crucial to explore the sorption mechanism of selenium species onto these two minerals on

the molecular scale by molecular modelling methods, for example, based on Density Function Theory (DFT).

In order to obtain molecular level information about the reaction mechanisms, it is possible to utilise quantum mechanic (QM) techniques for molecular modelling. Those have been widely used to estimate chemical reactions, properties of solid materials, and adsorption behaviour of molecules on solid surfaces. Nowadays, rather complex cluster or periodic model systems can be calculated, which enables e.g. clay-cation (Ren *et al.*, 2012; Tribe *et al.*, 2012) and even clay-cation-water (Seppälä *et al.*, 2016 and 2017) interaction studies. Typically, molecular modelling has been applied in connection with surface characterization like X-ray photoelectron spectroscopy (Ebina *et al.*, 1999) and extended X-ray absorption fine structure (Hattori *et al.*, 2009). Also, relation between QM and surface complexation modelling (SCM) has been formulated (Wesolowski *et al.*, 2009).

In the present study, QM and SCM were used in connection with the titration and sorption experiments to clarify the sorption mechanisms of Se(IV) and Se(VI) species onto phlogopite and calcite at the molecular level. The role of basal and edge surface sites of the minerals was taken into account in the sorption geometry and energy studies. The results of molecular modelling, namely the amount of weak sorption sites, were used for PHREEQC modelling on sorption isotherms of Se(IV) on phlogopite. The combined results assist to understand the chemical processes affecting the migration of selenium in the bedrock.

2. Materials and methods

Two types of sorbent materials, biotite and calcite, were investigated in this study. Biotite is a common phyllosilicate mineral with the approximate chemical formula,

$K(Mg,Fe)_3AlSi_3O_{10}(OH,F)_2$. It has a prismatic and sheet-like structure, where the negatively charged layers are connected to each other by potassium cation layers. Phlogopite is the Mg-endmember of biotite with the general chemical formula $KMg_3AlSi_3O_{10}(F,OH)_2$ where all the iron ions have been substituted by Mg (Figure 1a). Calcite ($CaCO_3$) has a hexagonal layered structure where calcium ions are located between the carbonate layers (Figure 1b).

The molecular modelling methods based on density functional theory (DFT) were used to investigate the crystalline and surface structures of phlogopite and calcite, and the sorption of selenium species onto these mineral surfaces. In the case of phlogopite, both the basal (001) and edge (110) surfaces were considered, because different types of sorption sites are believed to exist on these surfaces (Kyllönen et al., 2014), while in the case of calcite, the (104) surface was considered because of the homogeneity of its structure.

The calculations were performed with the CASTEP (CAmbridge Serial Total Energy Package) by Clark et al. (2009) code implemented into Materials Studio versions 8.0. CASTEP is a full-featured materials modelling code based on a first-principles quantum mechanical description of electrons and nuclei, and it has been designed specifically for solid-state materials science. It employs the density functional theory plane-wave pseudopotential method, which allows to perform first-principles quantum mechanics calculations that explore the properties of crystals and surfaces in materials such as semiconductors, ceramics, zeolites, metals, and minerals. Typical applications involve studies of surface chemistry, structural properties, band structure, density of states, and optical properties.

The modelling is based on three-dimensional atomistic models and solving the total electronic energy and overall electronic density distribution in order to define energetically stable structures for minerals and sorbing species (Leach, 2001). In the present study, the exchange-correlation

was described with generalized gradient approximation GGA-PBE. As a compromise between the accuracy and computational time of calculations, the ultrasoft pseudopotentials were used for each element. The potentials used were Al_00PBE.usp for aluminium, C_00PBE.usp for carbon, Ca_00PBE.usp for calcium, H_00PBE.usp for hydrogen, K_00PBE.usp for potassium, Mg_00.usp for magnesium, O_soft00.usp for oxygen, Se_00.usp for selenium, and Si_soft00.usp for silicon. The kinetic cut-off energy for a plane wave expansion of the wave function was 280 eV for calcite models, and 310 eV for phlogopite models. The cut-off values correspond fine quality for all the atoms, except for magnesium.

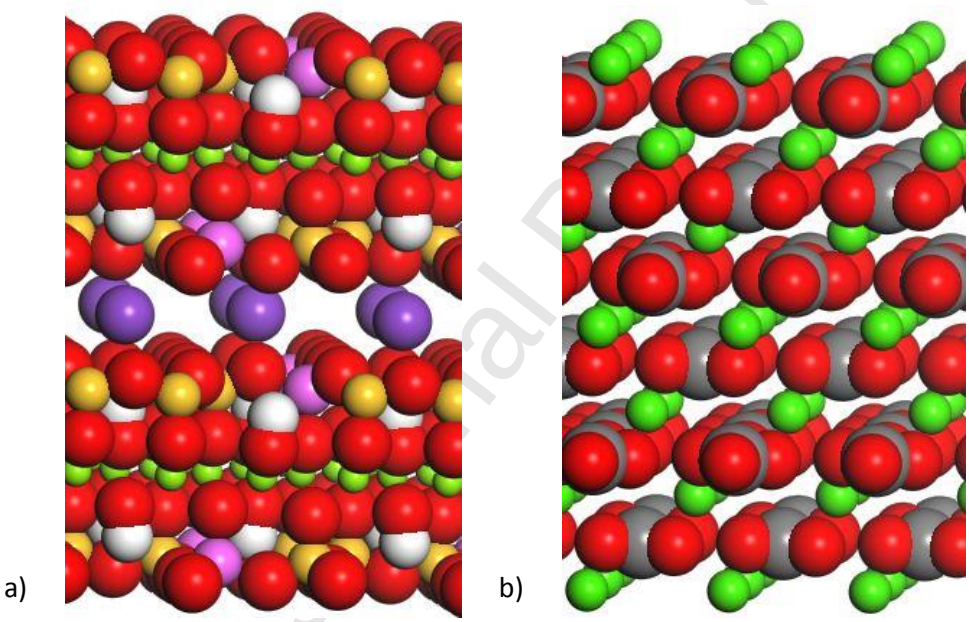


Figure 1. The layered structure of a) phlogopite; H – white, Na – purple, O – red, Si – yellow, Mg – green and b) calcite; Al – pink, C – grey, Ca – green.

3. Results

3.1 Optimization of mineral structures

The modelling studies start by optimizing the unit cell structures of minerals in order to validate modelling results with experimental ones. By this way, the description of the periodicity of the mineral bulk structures can be confirmed. The optimized crystal structures of phlogopite and calcite are shown in Figure 1. The lattice parameters of the energetically stable structure of phlogopite was calculated based on our earlier density functional calculations (Puhakka and Olin, 2014) of biotite which has about twice the unit cell as phlogopite. The optimized lattice parameters of the unit cell of phlogopite are a = 520.2 pm, b = 905.1 pm, c = 1 036.4 pm, and c/a = 1.992, when the Si:Al ratio is 3:1. Phlogopite is composed of a sheet-like structure that consists of negatively and positively charged layers. The negatively charged layers consist of tetrahedral (T) and octahedral (O) sheets that stack together to form 2:1 (TOT) layers with a characteristic repeat distance between two layers (Velde and Meunier, 2008). These negatively charged layers are balanced by cations which are exchangeable to cations in the external solution. Especially, the cations located in the edge of the interlayer of the sheet structure are sensitive for cation exchange reactions.

Calcite has also a layered structure where calcium ions are located between the carbonate layers. The optimized lattice parameters of the unit cell of calcite are a = b = 506.0 pm, c = 1 717.1 pm, and c/a = 3.393.

The optimized crystal structures of phlogopite and calcite were utilized to generate optimized surface structures which are typical for each mineral. In the case of phlogopite, the interest was on both basal and edge surfaces. Thus, both the (001) surface which is a typical basal surface

Journal Pre-proof

(terminated by potassium ions) and the (110) surface as an edge surface were studied in the DFT modelling for sorption of Se(IV) and Se(VI) on phlogopite surfaces.

The size of the surface cell in simulation for the phlogopite (110) surface model was 2.16 nm^2 (2 072.7 pm × 1 043.2 pm). The total thickness of the surface model was 0.98 nm, of which the layer of 0.49 nm was allowed to relax during the optimizing of the surface structure. The surface was hydrated and the $Si\text{-}O^-$ and $Al\text{-}O^-$ groups were ended by protons (H^+) in order to stabilize the surface structures. An empty void perpendicular to the surface was 0.8 nm.

The size of the surface cell in simulation for the phlogopite (001) surface model was 0.94 nm^2 (1 040.4 pm × 905.1 pm). The total thickness of the surface model was 1.87 nm, of which the layer of 1.20 nm was allowed to relax during the optimizing of the surface structure. An empty void perpendicular to the surface was 1.0 nm.

Calcite has three dominant surface structures, (10-2), (104) and (006). Of these surfaces, the (006) and (10-2) are terminated by calcium ions. On the (006) surface, the carbonate groups have planar orientation, and on the (10-2) surface, they are diagonal oriented groups. On the (104) surface, the carbonate groups are also diagonal oriented, but now the calcium ions are parallel to the carbonate groups. Thus, the (104) surface was selected for sorption studies, because its structure resembles the edge surface of phlogopite.

The size of the surface cell in simulation for the calcite (104) surface model was 1.66 nm^2 (1 635.9 pm × 1 012.1 pm). The total thickness of the surface model was 1.70 nm, of which the layer of 1.13 nm was allowed to relax during the optimizing of the surface structure. In the perpendicular direction to the surface, an empty void was 2.0 nm.

Journal Pre-proof

3.2 Sorption of Se(IV) species

Sorption studies onto the edge (110) and basal (001) surfaces of phlogopite and the (104) surface of calcite were performed with three Se(IV) species: SeO_3^{2-}, $HSeO_3^-$ and H_2SeO_3. On the edge surface of phlogopite, it was supposed that the sorption position is above the interlayer space of phlogopite. In the study, the bonding form of the Se species with the surface oxyanion was also considered. Two forms of bonding exist between the Se species and oxyanion atom on the mineral surfaces; via an oxygen atom or a selenium atom. In all of the studied cases, Se species was located onto the surface, and the uppermost surface structure of phlogopite or calcite was optimized together with Se species. Thus, the effect of initial positions of the Se species on the final sorption geometry was minimised. An empty void perpendicular to the surface was 1.0 nm.

The optimized bonding geometries of Se(IV) species on the phlogopite (110) surface are presented in Figure 2. The sorption of SeO_3^{2-} ion onto the phlogopite (110) surface via its oxygen atoms to the hydrogen atoms of the surface hydroxyl groups is shown in Figure 2a. If the sorption happens via a selenium atom of the oxyanion, SeO_3^{2-} takes a hydrogen atom from the surface hydroxyl group, and SeO_3^{2-} changes to $HSeO_3^-$ species (Figure 2b).

The sorption of $HSeO_3^-$ that happens via an oxygen atom of the oxyanion is shown in Figure 2c. During the sorption reaction, $HSeO_3^-$ gives up its oxygen atom to the surface and after the replacement of the surface hydroxyl groups, the reaction releases water like the S_N2-I reaction mechanism predicts (Chubar et al., 2005), and then $HSeO_3^-$ transfers to the cationic $HSeO_2^+$ species. If the sorption occurs via its selenium atom, there is no speciation change (Figure 2d).

When neutral H_2SeO_3 species adsorbs onto the surface, cationic $HSeO_2^+$ species forms and water releases, and the sorption of the species happens via an oxygen atom of the oxyanion (Figure 2e).

If the sorption reaction happens via a selenium atom, there is no changes in the Se species (Figure 2f). The results reveal that electron transfer reactions happen between the phlogopite surface and Se species. During these reactions, anionic or neutral Se species can transfer to cationic species, $HSeO_2^+$, on the edge surface of phlogopite. The $HSeO_2^+$ species can be an activated species during the complexation reaction. Sorption energies are listed in Table 1.

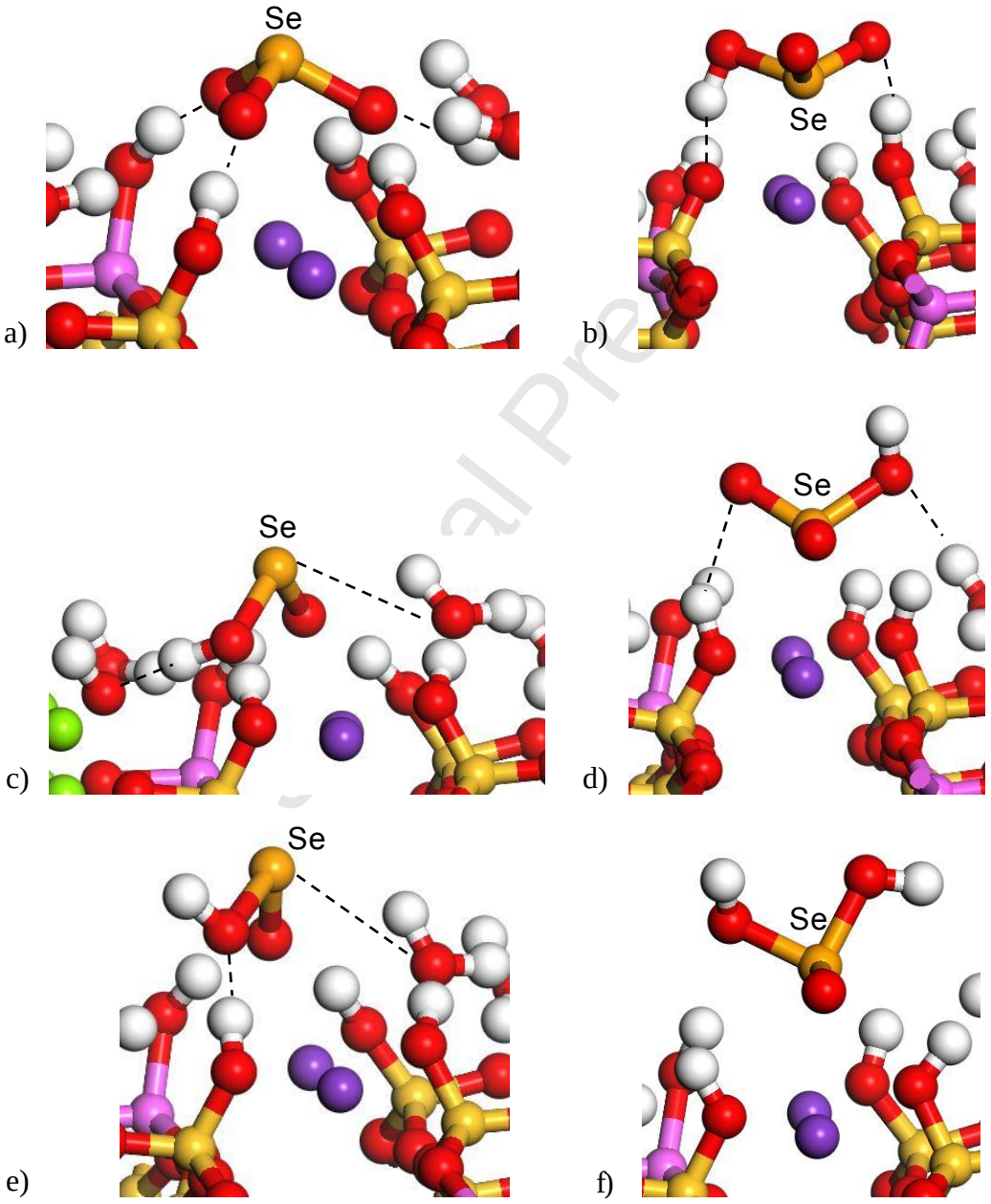


Figure 2. Sorption of SeO_3^{2-} (a and b), $HSeO_3^-$ (c and d) and H_2SeO_3 (e and f) onto the phlogopite (110) surface. Al – pink, H – white, Na – purple, O – red, Si – yellow, Mg – green.

The optimized bonding geometries of Se(IV) species on the phlogopite (001) surface are presented in Figure 3. In these cases, an empty void of 1.5 nm perpendicular of the surface models was set. The calculations show that the sorption of SeO_3^{2-} happens via its oxygen atoms to the potassium ions of the surface (Figure 3a). The sorption reaction corresponds to $HSeO_3^-$ species (Figure 3b), and no chemical changes occurs during the sorption. When neutral H_2SeO_3 species adsorbs onto the surface, then cationic $HSeO_2^+$ species forms (Figure 3c), the same as the sorption reaction onto the phlogopite (110) surface. In these cases, the coordination direction of the Se species have not been taken into account. However, the results reveal that electron transfer reactions take place on the basal surface of the phlogopite, but the reactions are not so dominant as on the edge surface. Sorption energies are listed in Table 1.

Journal Pre-proof

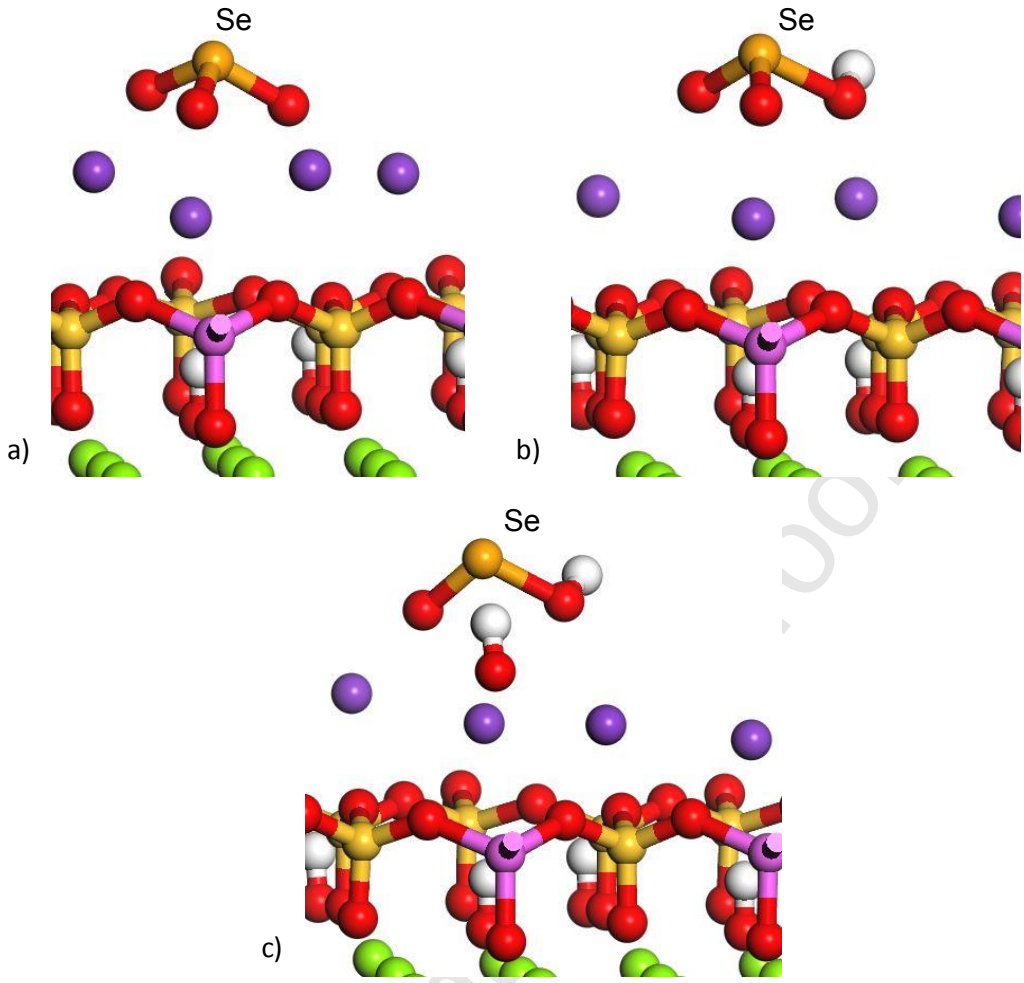


Figure 3. Sorption of SeO_3^{2-} (a), $HSeO_3^-$ (b) and H_2SeO_3 (c) onto the phlogopite (001) surface. Al – pink, H – white, Na – purple, O – red, Si – yellow, Mg – green.

In Figure 4, the optimized bonding geometries of Se(IV) species on the calcite (104) surface are presented. The calculation results show that, in these cases, all three investigated Se species (SeO_3^{2-}, $HSeO_3^-$ and H_2SeO_3) attach to the surface via physical interactions without surface complexation reactions happening. The sorption geometry of SeO_3^{2-} and $HSeO_3^-$ is very similar on the calcite (104) surface and the phlogopite (001) surface, and sorption energies are listed in Table 1.

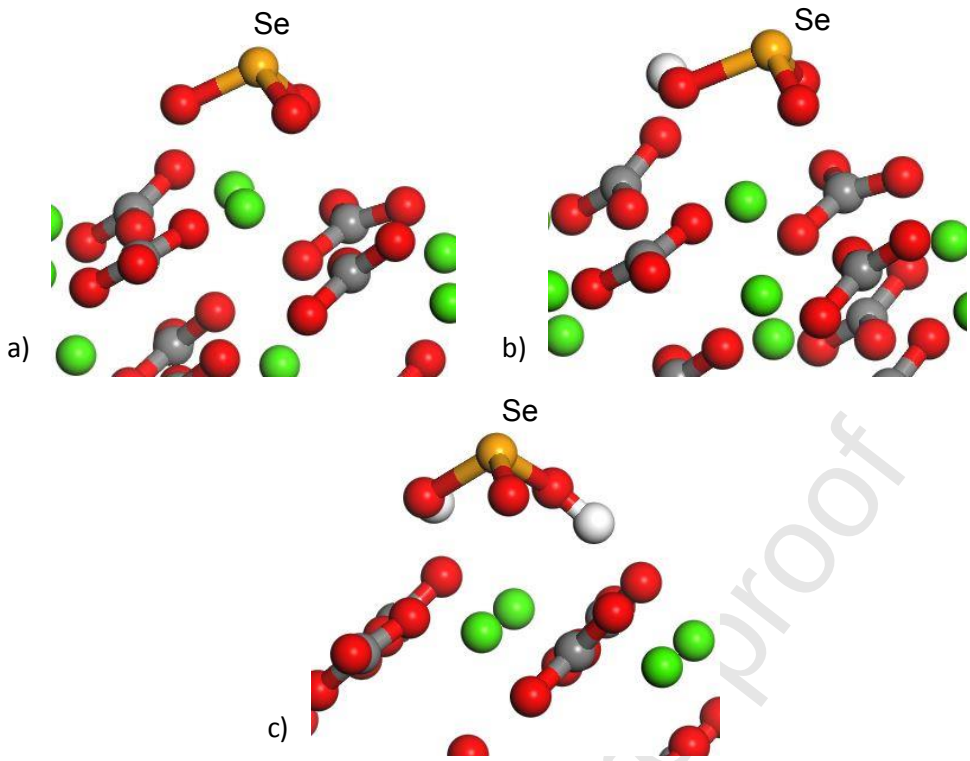


Figure 4. Sorption of SeO_3^{2-} (a), $HSeO_3^-$ (b) and H_2SeO_3 (c) onto the calcite (104) surface. C – carbon, Ca – green, H – white, O – red.

3.3 Sorption of Se(VI) species

In the case of the Se(VI) species, the coordination of the Se species via the oxygen atoms was only considered, because according to the calculated sorption energies for the Se(IV) species (Table 1), the sorption via the oxygen atoms is energetically more favourable than the sorption via the Se atom. The optimized bonding geometries of Se(VI) species on the phlogopite (110) surface are presented in Figure 5. In these cases, an empty void of 2.0 nm perpendicular to the surface models was set. The results show that the sorption of SeO_4^{2-} onto the phlogopite (001) surface happens via its oxygen atoms to the hydrogen atoms of the surface hydroxyl groups (Figure 5a). During the sorption of $HSeO_4^-$ (Figure 5b), it gives up its oxygen atom, and reacts with the hydrogen atoms of the surface hydroxyl groups forming a water molecule like in the

case of $HSeO_3^-$ species. As a consequence of the reaction, $HSeO_3^-$ species forms (Figure 5c). When neutral H_2SeO_4 species adsorbs onto the surface, it also gives up its oxygen atom, as a consequence, the $HSeO_3^-$ species forms (Figure 5e). The results reveal that electron transfer reactions happen between the phlogopite (110) surface and the Se(VI) species, like in the case of Se(IV) species.

Journal Pre-proof

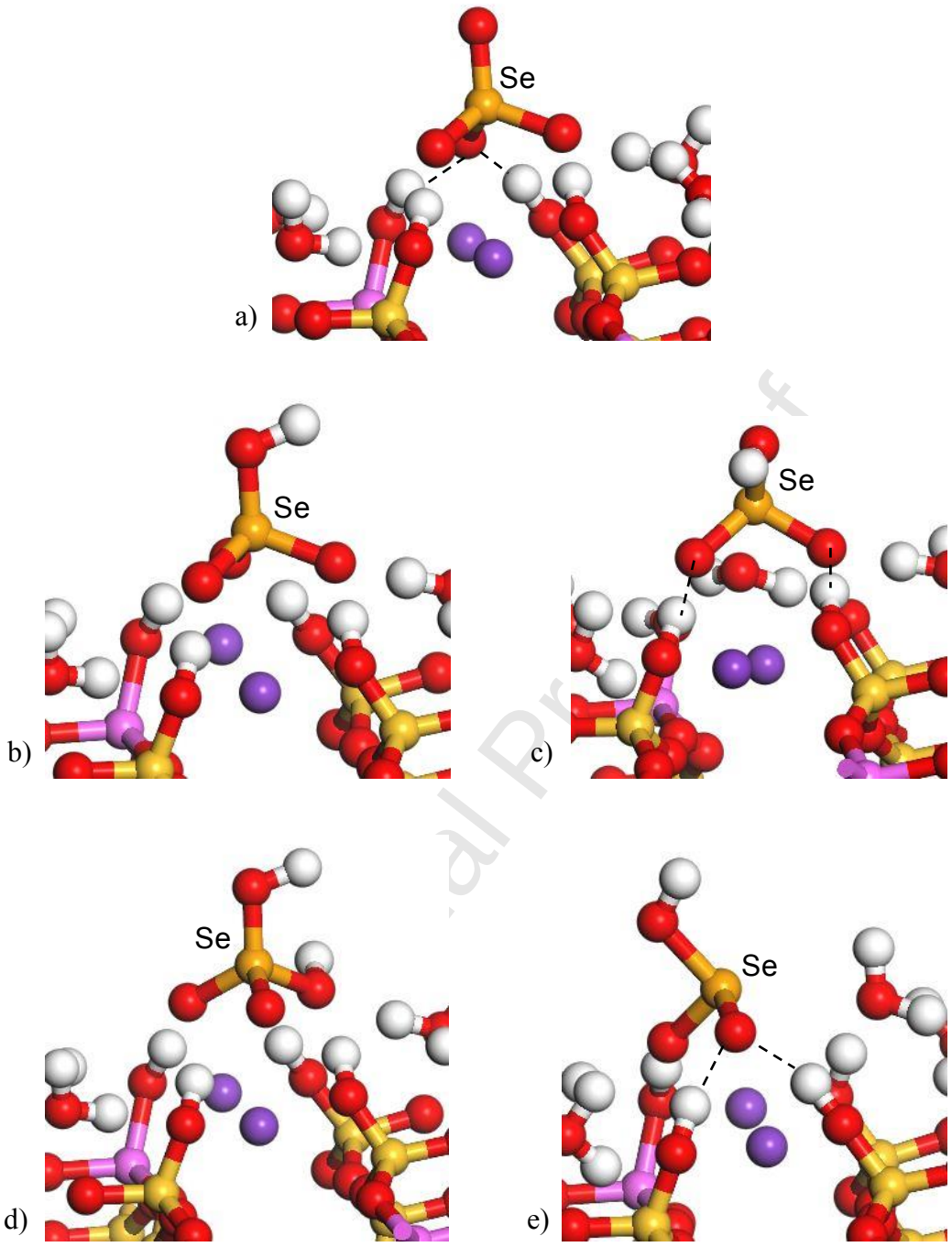
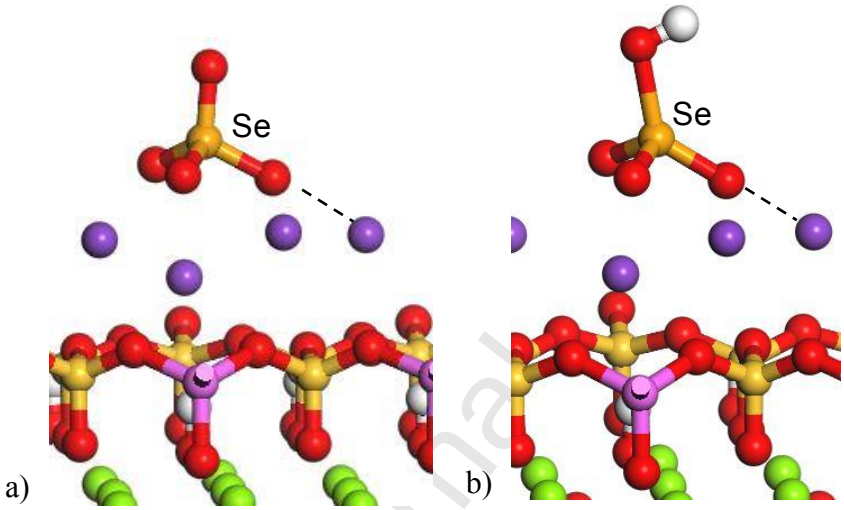


Figure 5. Sorption of SeO_4^{2-} (a), $HSeO_4^-$ (b) and H_2SeO_4 (d) onto the phlogopite (110) surface. In the case of $HSeO_4^-$ and H_2SeO_4, changes in the chemical composition of the Se species happen during the sorption, and the final sorption products are also presented (c and e), respectively. Al – pink, H – white, Na – purple, O – red, Si – yellow.

The optimized bonding geometries of Se(VI) species on the phlogopite (001) surface are presented in Figure 6. Sorption of SeO_4^{2-} takes place via its oxygen atoms to the potassium ions of the surface (Figure 6a). The sorption reaction of $HSeO_4^-$ happens in a similar way (Figure 6b) with chemical changes occurring during the sorption process and the $HSeO_4^-$ ions disorders only slightly. When neutral H_2SeO_4 species adsorbs onto the surface, the dissociation reaction happens with releasing a hydroxyl group which forms an ionic bonding with the potassium ions of the surface (Figure 6c).



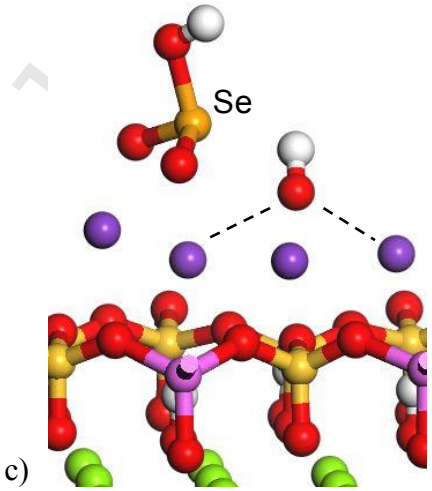


Figure 6. Sorption of SeO_4^{2-} (a), $HSeO_4^-$ (b) and H_2SeO_4 (c) onto the phlogopite (001) surface. Al – pink, H – white, Na – purple, O – red, Si – yellow, Mg – green.

The optimized bonding geometries of Se(VI) species on the calcite (104) surface are presented in Figure 7. Like in the case of Se(IV) species (Figure 4), all the investigated Se species (SeO_4^{2-}, $HSeO_4^-$ and H_2SeO_4) attach to the surface via physical interactions, and no surface complexation reactions happen. The sorption happens via the oxygen atoms, and sorption energies are listed in Table 1.

Journal Pre-proof

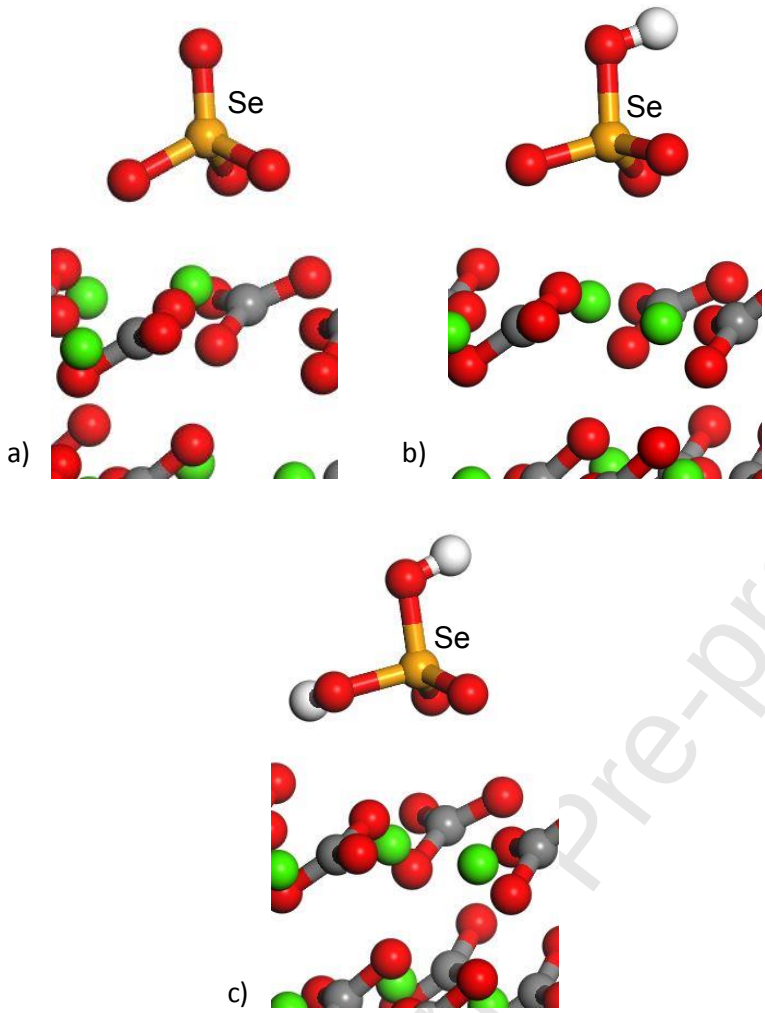


Figure 7. Sorption of SeO_4^{2-} (a), $HSeO_4^-$ (b) and H_2SeO_4 (c) onto the calcite (104) surface. C – carbon, Ca – green, H – white, O – red.

3.4 Sorption energies

The energies for surface reactions of Se species on the phlogopite (110) and (001) surfaces and the calcite (104) surface are presented in Table 1. The results indicate that Se species attach to the surface via oxygen atom of the oxyanion. Exothermic sorption energies for $HSeO_3^-$, $HSeO_4^-$, H_2SeO_3 and H_2SeO_4 on the phlogopite (110) surface indicate that surface complexation reactions are very presumable on the edge surfaces of phlogopite (Figures 2c, 2e, 5c and 5e) compared to

Journal Pre-proof

the basal (001) surfaces. On the calcite surface, ion exchange reactions are possible only for neutral Se species, H_2SeO_3 and H_2SeO_4 (Figs. 4c and 7c). Though the neutral H_2SeO_3 and H_2SeO_4 seem to form the very stable complexes on the edge surfaces of phlogopite, it has to be stated that these neutral Se species do not occur in the natural groundwater conditions in the bedrock of a nuclear waste repository (Lehto and Hou, 2011). Therefore, the most presumable Se species in the sorption reactions that happen under the geological conditions of a nuclear waste repository are $HSeO_3^-$ and $HSeO_4^-$.

Table 1. Sorption energies (eV) of the Se species onto the phlogopite and calcite surfaces.

Se species	Phlogopite			Calcite
	(110)	(110)	(001)	(104)
	–O–Se	–Se–O	–O–Se	–O–Se
$Se(IV)O_3^{2-}$	4.6	6.4	5.7	10.1
$Se(VI)O_4^{2-}$	4.9		6.6	7.3
$HSe(IV)O_3^-$	-1.8	4.5	3.4	5.1
$HSe(VI)O_4^-$	-1.3		1.4	4.0
$H_2Se(IV)O_3$	-5.2	0.7	-2.3	0.1
$H_2Se(VI)O_4$	-6.6		-3.5	0.6

3.5 Surface site density estimations

In addition to the calculation of the sorption energies, the calculated sorption geometries were utilized to estimate the number of surface sites for sorption of Se species on both of the

phlogopite surfaces. In Figure 8, the top views of the surface models for the basal (001) and edge (110) surfaces of phlogopite with $HSeO_3^-$ species are presented.

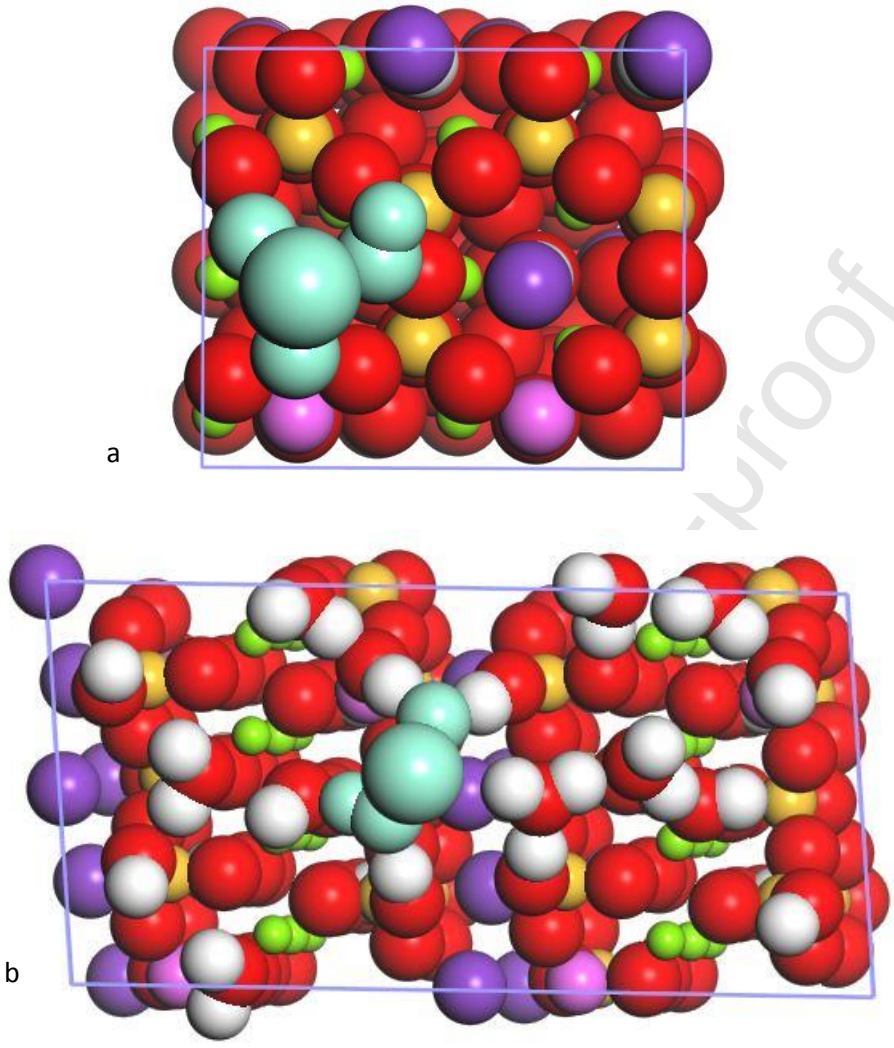


Figure 8. Phlogopite: a) the (001) and b) (110) surface. Al – pink, H – white, Na – purple, O – red, Si – yellow, Mg – green, Se species – turquoise.

In the case of the phlogopite (001) surface (Figure 8a), the surface area of the model is 0.94 nm^2. When the maximum coverage of the surface model caused by $HSeO_3^-$ species is considered, there can be approximately three Se species attached onto the model. Based on this assumption, the site density of $HSeO_3^-$ on the basal surface is estimated to be 3.2 sites/nm^2.

On the phlogopite (110) edge surface (Figure 8b), the selenium species $HSeO_2^+$ is adsorbed above the interlayer of phlogopite which is supposed to be the significant edge position. The area of the surface model is 2.16 nm^2, and if it is supposed that all of this kind of surface sites are occupied, there can be approximately three selenium species on the surface model. Based on this assumption, the maximum site density of the phlogopite edge surface is estimated to be 1.4 sites/nm^2.

4. Discussion

The surface site density values estimated from this work (1.4 sites/nm^2 for edge sites and 3.2 sites/nm^2 for basal sites) is in accordance with the experimental data from other studies. For example, the recommended surface site density for all minerals by Davis and Kent (1990) is 2.31 sites/nm^2 and this general value was used in many surface modelling studies (Baeyens and Bradbury, 1997, 1995; Ervanne et al., 2013). However, this value is too general without the consideration of the mineral types and surface differences. The surface density values estimated from this work are more specific taking into account the different properties of the phlogopite (001) and (110) surfaces.

The estimated surface site density values were used in our PHREEQC modelling based on titration, sorption edge and sorption isotherm experimental results of Se(IV) sorption on phlogopite (Li et al., 2018; Li et al., 2019). A multi-site surface complexation model was successfully developed by treating the (001) and (110) surfaces as weak sorption sites in combination with strong sorption sites with a low site density (0.00068 sites/nm^2). The multi-site surface complexation model was validated to describe the Se(IV) sorption on phlogopite over a pH range from at least 7.5 to 9.5 which covers typical groundwater pH ranges found in host rocks suitable for of nuclear waste repositories (Figure 9).

The selectivity coefficients (logK values) of different selenium species (SeO_3^{2-}, $HSeO_3^-$, $HSeO_3^-$ - H^+, H_2SeO_3 – H^+) were deduced from PHREEQC modelling with the order $logK(SeO_3^{2-}) < logK(HSeO_3^-) < logK(HSeO_3^- - H^+) < logK(H_2SeO_3 – H^+)$ (Li et al., 2019). This result is in accordance with the determined sorption energies of different Se species by DFT modelling (Section 3.4 and Table 1). Both the molecular modelling and PHREEQC modelling results show that H_2SeO_3 could form the most stable complexes on the surface of phlogopite while SeO_3^{2-} is the least presumable Se species considering surface complexation on phlogopite.

Mechanistic understanding of the sorption processes on the mineral surfaces can be studied by combining molecular modelling and surface complexation modelling with PHREEQC. The molecular modelling results can strengthen the understanding of the properties of the assumed two weak sorption sites in the PHREEQC model. These two weak sorption sites are cation exchange and surface complexation sites. The cation exchange reactions happen on the basal surfaces of phlogopite and the reactions are based on the ionic forces. The surface complexation reactions occur on the edge surfaces and the reactions are based on the hydrogen bonding between the Se species and the mineral surfaces.

PHREEQC modelling on the sorption isotherm curve (Figure 9) gives information of reactions on the mineral surfaces. The modelling results also suggest the existence of strong sorption sites. The properties of the deduced strong sorption sites from the multi-site surface complexation model is still under discussion (Dähn et al, 2011). However, the PHREEQC modelling results show that the existence of the strong sorption sites are essential for the accurate simulation of the whole sorption isotherm curve, especially in the low concentration area ($< 10^{-7}$ M) where the sorption of Se(IV) ions is dominated by the strong sorption sites. Our results are corroborated by the work of Dähn et al (2011) where polarized extended X-ray absorption fine structure (P-

EXAFS) method was applied to study the nature of the strong sorption sites in the case of Zn sorption on montmorillonite. Their results show that strong sorption occurs on the mineral surface as a mixture of surface complexes bound to the edge sites of the cis-vacant (cv) and trans-vacant (tv) of Al octahedrons. P-EXAFS studies are needed to understand the true nature of the so called "strong" sorption sites in the case of Se(IV) sorption on phlogopite.

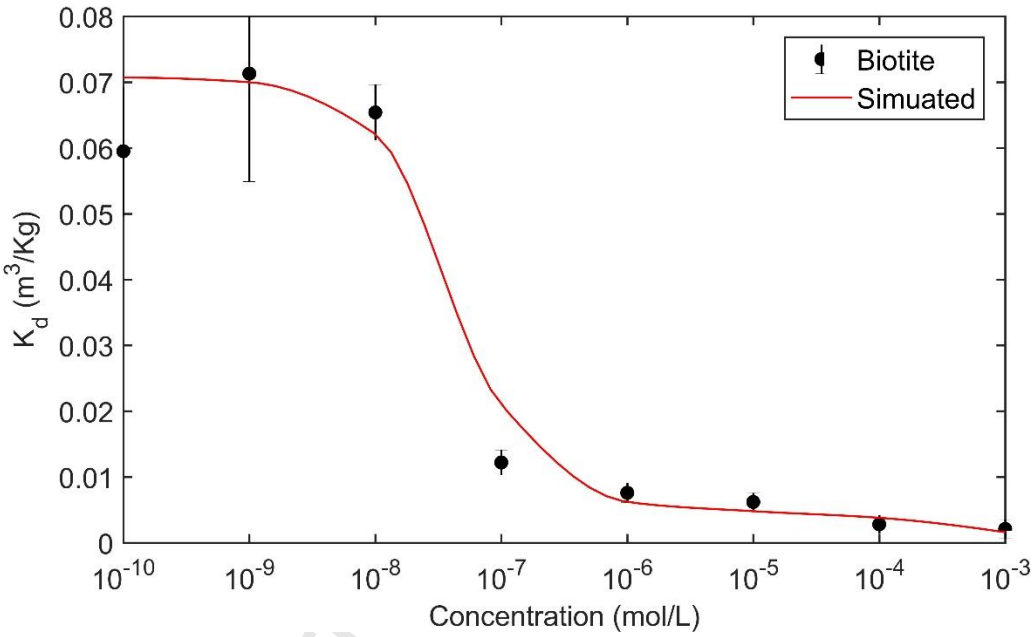


Figure 9. Experimental data of Se(IV) sorption on biotite in Grimsel groundwater simulant as a function of Se concentration from 10^{-10} M to 10^{-3} M and the continuous line is the simulated data with surface complexation model (Li et al., 2018).

5. Conclusions

In this research, the sorption properties of selenium on phlogopite and calcite were studied because these minerals have a potential role to sorb radioactive elements in crystalline bedrock from nuclear waste, and therefore have a strong impact on the migration of radionuclides. The results of the sorption studies of Se(IV) and Se(VI) species reveal that during the sorption

process, electron transfer reactions happen between the phlogopite surface and Se species, and surface complexation reactions happen on the edge surfaces of phlogopite. During these reactions, anionic or neutral Se(IV) species can transfer to cationic species, $HSeO_2^+$. On the basal surfaces of phlogopite, the cation exchange reactions happen like on the calcite surfaces.

The calculated results of the surface reaction energies of Se(IV) and Se(VI) species on phlogopite and calcite surfaces reveal that neutral H_2SeO_3 and H_2SeO_4 can form the most stable complexes on mineral surfaces whereas SeO_3^{2-} or SeO_4^{2-} are the least reactive species. This result is consistent with the selectivity coefficients of different surface reactions deduced from the multi-site surface complexation model which describes successfully Se(IV) sorption on the surface of phlogopite.

The sorption geometries were utilized to estimate the surface site densities on both phlogopite surfaces. The estimated surface site densities of the basal and edge phlogopite surfaces are 3.2 sites/nm^2 and 1.4 sites/nm^2, respectively. These surface site density data were used in the development of the multi-site surface complexation model as weak sorption sites. In addition, a strong sorption site was deduced from the multi-site surface complexation model with very low site density. The nature of the strong sorption site in the case of Se sorption on phlogopite or calcite is still unclear and more investigations, like P-EXAFS measurements, are needed to interpret the physical property of the strong sorption site. Our results show that mechanistic understanding of the sorption processes on the mineral surfaces can be elucidated through a combination of molecular and surface complexation modelling.

Journal Pre-proof

Acknowledgements

The research leading to these results has received funding from The Finnish Research Programme on Nuclear Waste Management KYT2018. Further, the authors wish to acknowledge CSC – IT Center for Science, Finland, for computational resources.

References

Aaltonen, I., Engström, J., Front, K., Gehör, S., Kosunen, P., Kärki, A., Paananen, M., Paulamäki, S., Mattila, J., 2016. Geology of Olkiluoto (No. POSIVA Report 2016-16).

Appelo, C.A.J., Postma, D., 2004. Geochemistry, Groundwater and Pollution. CRC Press.

Atwood, D.A., 2010. Radionuclides in the Environment. WILEY.

Baeyens, B., Bradbury, M.H., 1997. A mechanistic description of Ni and Zn sorption on Na-montmorillonite Part I: Titration and sorption measurements. Journal of Contaminant Hydrology 27, 199–222. https://doi.org/10.1016/S0169-7722(97)00008-9

Baeyens, B., Bradbury, M.H., 1995. A Quantitative Mechanistic Description of Ni, Zn and Ca Sorption on Na-Montmorillonite Part II: Sorption Measurements. TECHNICAL REPORT NTB 95-05, Nagra, Wettingen, Switzerland.

Boult, K.A., Cowper, M.M., Heath, T.G., Sato, H., Shibutani, T., Yui, M., 1998. Towards an understanding of the sorption of U(VI) and Se(IV) on sodium bentonite. Journal of Contaminant Hydrology 35, 141–150.

Chubar, N.I., Kanibolotskyy, V.A., Strelko, V.V., Gallios, G.G., Samanidou, V.F., Shaposhnikova, T.O., Milgrandt, V.G., Zhuravlev, I.Z., 2005. Adsorption of phosphate ions on

Journal Pre-proof

novel inorganic ion exchangers. Colloids and Surfaces A: Physicochemical and Engineering Aspects 255, 55–63. https://doi.org/10.1016/j.colsurfa.2004.12.015

Clark, S.J., Segall, M.D., Pickard, C.J., Hasnip, P.J., Probert, M.I.J., Refson, K., Payne, M.C., 2009. First principles methods using CASTEP. Zeitschrift für Kristallographie - Crystalline Materials 220, 567–570. https://doi.org/10.1524/zkri.220.5.567.65075

Dähn, R., Baeyens, B., Bradbury, M.H., 2011. Investigation of the different binding edge sites for Zn on montmorillonite using P-EXAFS – The strong/weak site concept in the 2SPNE SC/CE sorption model. Geochimica et Cosmochimica Acta 75, 5154–5168. https://doi.org/10.1016/j.gca.2011.06.025

Davis, J.A., Kent, D.B., 1990. Surface Energy and Adsorption at Mineral/Water Interfaces: An Introduction. Mineral-Water Interface Geochemistry, Reviews in Mineralogy 23, 177–260.

De Cannière, P., Maes, A., Williams, S., Bruggeman, C., Beauwens, T., Maes, N., Cowper, M., 2010. Behaviour of Selenium in Boom Clay. Work performed under contract: SCK•CEN ref: CO 90 01 1467.01 1467 RP.W&D.037 – NIROND ref: CCHO2004/00/00 DS251-A44/2.1. External Report of the Belgian Nuclear Research Centre, SCK•CEN-ER-120.

Duc, M., Lefevre, G., Fedoroff, M., Jeanjean, J., Rouchaud, J.C., Monteil-Rivera, F., Dumonceau, J., Milonjic, S., 2003. Sorption of selenium anionic species on apatites and iron oxides from aqueous solutions. Journal of Environmental Radioactivity 70, 61–72. https://doi.org/10.1016/s0265-931x(03)00125-5

Ebina T., Iwasaki T., Onodera Y., Chatterjee, 1999. A comparative study of DFT and XPS with reference to the adsorption of caesium ions in smectites. Computational Materials Science 14, 254-260.

Journal Pre-proof

Eikenberg, J., Hoehn, E., Fierz, T., U.Frick, 1994. Grimsel Test Site: Preparation and performance of migration experiments with radioisotoQS of sodium, strontium and iodine.

Ervanne, H., Hakanen, M., Lehto, J., 2016. Selenium sorption on clays in synthetic groundwaters representing crystalline bedrock conditions. J Radioanal Nucl Chem 307, 1365–1373. https://doi.org/10.1007/s10967-015-4254-7

Ervanne, H., Puukko, E., Hakanen, M., 2013. Modeling of Sorption of Eu, Mo, Nb, Ni, Pa, Se, Sn, Th and U on Kaolinite and Illite in Olkiluoto Groundwater Simulants. Laboratory of Radiochemitry, Department of Chemistry, University of Helsinki.

Ewing, R.C., 2015. Long-term storage of spent nuclear fuel. Nature Materials 14, 252–257.

Geier, J., Bath, A., Stephansson, O., 2012. Comparison of site descriptive models for Olkiluoto, Finland and Forsmark, Sweden (No. STUK-TR 14).

Grisak, G.E., Pickens, J.F., 1980. Solute transport through fractured media: 1. The effect of matrix diffusion. Water Resources Research 16, 719–730.

Hattori T., Saito T., Ishida K., Scheinost A.C., Tsuneda T., Nagasaki S., Tanaka S., 2009 The structure of monomeric and dimeric uranyl adsorption complexes on gibbsite: A combined DFT and EXAFS study. Geochimica et Cosmochimica Acta 73, 5975-5988.

Hayes, K.F., Roe, A.L., Brown, G.E., Hodgson, K.O., Leckie, J.O., Parks, G.A., 1987. In Situ X-ray Absorption Study of Surface Complexes: Selenium Oxyanions on α-FeOOH. Science 238, 783–786. https://doi.org/10.1126/science.238.4828.783

Ikonen, J., Sardini, P., Jokelainen, L., Siitari-Kauppi, M., Martin, A., Eikenberg, J., 2016a. The tritiated water and iodine migration in situ in Grimsel granodiorite. Part I: determination of the

Journal Pre-proof

diffusion profiles. Journal of Radioanalytical and Nuclear Chemistry 310, 1041–1048. https://doi.org/10.1007/s10967-016-4890-6

Ikonen, J., Voutilainen, M., Söderlund, M., Jokelainen, L., Siitari-Kauppi, M., Martin, A., 2016b. Sorption and diffusion of selenium oxyanions in granitic rock. J Contam Hydrol 192, 203–211. https://doi.org/10.1016/j.jconhyd.2016.08.003

Jokelainen, L., Meski, T., Lindberg, A., Soler, J.M., Siitari-Kauppi, M., Martin, A., Eikenberg, J., 2013. The determination of 134Cs and 22Na diffusion profiles in granodiorite using gamma spectroscopy. Journal of Radioanalytical and Nuclear Chemistry 295, 2153–2161. https://doi.org/10.1007/s10967-012-2268-y

Kyllönen, J., Hakanen, M., Lindberg, A., Harjula, R., Vehkamäki, M., Lehto, J., 2014. Modeling of cesium sorption on biotite using cation exchange selectivity coefficients. Radiochimica Acta 102, 919–929. https://doi.org/10.1515/ract-2013-2180

Leach, A.R., 2001. Molecular Modelling: Principles and Applications, 2nd ed. Pearson Education.

Lehto, J., Hou, X., 2011. Chemistry and Analysis of Radionuclides Laboratory Techiques and Methodology. WILEY-VCH.

Li, X., Puhakka, E., Ikonen, J., Söderlund, M., Lindberg, A., Holgersson, S., Martin, A., Siitari-Kauppi, M., 2018. Sorption of Se species on mineral surfaces, part I: Batch sorption and multi-site modelling. Applied Geochemistry 95, 147–157. https://doi.org/10.1016/j.apgeochem.2018.05.024

Journal Pre-proof

Li, X., Puhakka, E., Liu, L., Zhang, W., Ikonen, J., Lindberg, A., Siitari-Kauppi, M., 2019. Multi-site surface complexation modelling of Se(IV) sorption on biotite. (Manuscript)

Martínez, M., Giménez, J., de Pablo, J., Rovira, M., Duro, L., 2006. Sorption of selenium(IV) and selenium(VI) onto magnetite. Applied Surface Science 252, 3767–3773. https://doi.org/10.1016/j.apsusc.2005.05.067

Missana, T., Alonso, U., Garcia-Gutierrez, M., 2009a. Experimental study and modelling of selenite sorption onto illite and smectite clays. J Colloid Interface Sci 334, 132–138. https://doi.org/10.1016/j.jcis.2009.02.059

Missana, T., Alonso, U., Scheinost, A.C., Granizo, N., García-Gutiérrez, M., 2009b. Selenite retention by nanocrystalline magnetite: Role of adsorption, reduction and dissolution/co-precipitation processes. Geochimica et Cosmochimica Acta 73, 6205–6217. https://doi.org/10.1016/j.gca.2009.07.005

Möri, A., Alexander, W.R., Geckeis, H., Hauser, W., Schäfer, T., Eikenberg, J., Fierz, T., Degueldre, C., Missana, T., 2003. The colloid and radionuclide retardation experiment at the Grimsel Test Site: influence of bentonite colloids on radionuclide migration in a fractured rock. Colloids and Surfaces A: Physicochemical and Engineering Aspects 217, 33–47. https://doi.org/10.1016/S0927-7757(02)00556-3

Muuri, E., 2015. The sorption and diffusion of Ba-133 in granitic rocks (Master thesis). University of Helsinki, Finland.

Muuri, E., Siitari-Kauppi, M., Matara-aho, M., Ikonen, J., Lindberg, A., Qian, L., Koskinen, L., 2017. Cesium sorption and diffusion on crystalline rock: Olkiluoto case study. J Radioanal Nucl Chem 311, 439–446. https://doi.org/10.1007/s10967-016-5087-8

Journal Pre-proof

Neretnieks, I., 1980. Diffusion in the rock matrix: An important factor in radionuclide retardation? Journal of Geophysical Research: Solid Earth 85, 4379–4397. https://doi.org/10.1029/JB085iB08p04379

Posiva Oy, 2012. Safety Case for the Disposal of Spent Nuclear Fuel at Olkiluoto - Synhesis 2012 (No. POSIVA 2012-12).

Poteri, A., Nordman, H., Pulkkanen, V.-M., Smith, P., 2014. Radionuclide Transport in the Repository Near-Field and Far-Field. POSIVA 2014-02.

Puhakka, E., Olin, M., 2014. Ab Initio Studies on Cation Exchange and Surface Complexation Reactions on Biotite Surface, in: Final Workshop Proceedings of the Collaborative Project "Crystalline ROCK Retention Processes" (7th EC FP CP CROCK), KIT Scientific Report 7656, KIT Scientific Publishing, Karlsruhe. pp. 125–131. http://dx.doi.org/10.5445/KSP/1000037468

Ren X., Yang S., Tan X., Chen C., Sheng G., Wang X., 2012. Mutual effects of copper and phosphate on their interaction with γ-Al2O3: Combined batch macroscopic experiments with DFT calculations. Journal of Hazardous Materials 237-238, 199-208.

Séby, F., Potin-Gautier, M., Giffaut, E., Donard, O.F.X., 1998. Assessing the speciation and the biogeochemical processes affecting the mobility of selenium from a geological repository of radioactive wastesto the biosphere. Analusis 26, 193–198. https://doi.org/10.1051/analusis:1998134

Seppälä A., Puhakka E., Olin M., 2016. Effect of layer charge on the crystalline swelling of Na^{+}, K^{+} and Ca^{2+} montmorillonites: DFT and molecular dynamics studies. Clay Minerals 51, 197-211.

Journal Pre-proof

Söderlund, M., Hakanen, M., Lehto, J., 2016. Sorption of cesium on boreal forest soil I: the effect of grain size, organic matter and mineralogy. Journal of Radioanalytical and Nuclear Chemistry 309, 637–645. https://doi.org/10.1007/s10967-015-4612-5

Soler, J.M., Landa, J., Havlova, V., Tachi, Y., Ebina, T., Sardini, P., Siitari-Kauppi, M., Eikenberg, J., Martin, A.J., 2015. Comparative modeling of an in situ diffusion experiment in granite at the Grimsel Test Site. Journal of Contaminant Hydrology 179, 89–101. https://doi.org/10.1016/j.jconhyd.2015.06.002

Tachi, Y., Ebina, T., Takeda, C., Saito, T., Takahashi, H., Ohuchi, Y., Martin, A.J., 2015. Matrix diffusion and sorption of Cs+, Na+, I– and HTO in granodiorite: Laboratory-scale results and their extrapolation to the in situ condition. Journal of Contaminant Hydrology 179, 10–24. https://doi.org/10.1016/j.jconhyd.2015.05.003

Tribe L., Hinrichs R., Kubicki J.D., 2012. Adsorption of Nitrate on Kaolinite Surfaces: A Theoretical Study. The Journal of Physical Chemistry B 116, 11266-11273.

Tsai, S.C., Wang, T.H., Li, M.H., Wei, Y.Y., Teng, S.P., 2009. Cesium adsorption and distribution onto crushed granite under different physicochemical conditions. Journal of hazardous materials 161, 854–61. https://doi.org/10.1016/j.jhazmat.2008.04.044

Velde, B.B., Meunier, A., 2008. The Origin of Clay Minerals in Soils and Weathered Rocks. Springer-Verlag, Berlin Heidelberg.

Vilks, P., Degueldre, C., 1991. Sorption behaviour of 85Sr, 131Iand 137Cs on colloids and suspended particles from the Grimsel Test Site, Switzerland. Applied Geochemistry 6, 553–563.

Journal Pre-proof

Wesolowski, D.J., Bandura, A.V., Cummings, P.T., Fenter, P.A., Kubicki J.D., Lvov S.N., Machesky, M.L., Mamontov, E., Předota, M., Ridley, M.K., Rosenqvist, J., Sofo, J.O., Vlcek, L., Zhang, Z., 2009. Atomistic origins of mineral-water interfacial phenomena and their relation to surface complexation models. Geochimica et Cosmochimica Acta 73(13), A1429.

Yang, X., Ge, X., He, J., Wang, C., Qi, L., Wang, X., Liu, C., 2018. Effects of Mineral Compositions on Matrix Diffusion and Sorption of ^{75}Se(IV) in Granite. Environmental Science & Technology 52, 1320–1329. https://doi.org/10.1021/acs.est.7b05795

Journal Pre-proof

Declarations of interest: none

Journal Pre-proof

Journal Pre-proof

Highlights:

- Se(IV) and Se(VI) sorption on phlogopite and calcite were studied by DFT modelling
- Periodic systems, site densities and site types were calculated
- Surface complexations happen via hydrogen bonding on phlogopite edge surfaces
- Cation exchange reactions happen on phologopite basal surfaces
- Only cation exchange reactions are possible on calcite surfaces

Journal Pre-proof